ELSEVIER

Journal of Nuclear Materials 241–243 (1997) 678–683

journal of nuclear materials

The tungsten experiment in ASDEX Upgrade

R. Neu [a,*], K. Asmussen [a], S. Deschka [a], A. Thoma [a], M. Bessenrodt-Weberpals [a], R. Dux [a], W. Engelhardt [a], J.C. Fuchs [a], J. Gaffert [a], C. García-Rosales [b], A. Herrmann [a], K. Krieger [a], F. Mast [a], J. Roth [a], V. Rohde [a], M. Weinlich [a], U. Wenzel [a], ASDEX Upgrade Team [a], ASDEX NI-Team [a]

[a] *Max-Planck-Institut für Plasmaphysik, IPP-EURATOM Association, D-85748 Garching and D-10117 Berlin, Germany*
[b] *CEIT, 20009 San Sebastian, Spain*

Abstract

Tungsten coated tiles, manufactured by plasma spray on graphite, were mounted in the divertor of the ASDEX Upgrade tokamak and cover almost 90% of the surface facing the plasma in the strike zone. Over 500 plasma discharges, among which around 300 were heated with heating powers up to 10 MW, were performed up to now. The tungsten flux in the divertor was monitored by a WI line at 400.8 nm. In the plasma centre an array of spectral lines at 5 nm emitted by ionisation states around W XXX was monitored. Under normal discharge conditions W-concentrations of around 10^{-5} or even lower were found. The influence on the main plasma parameters was negligible. In a few low power discharges accumulation of tungsten occurred and the temperature profile was flattened. The concentrations of the intrinsic impurities carbon and oxygen are comparable to the discharges with graphite divertor. Furthermore, the density-limits and the β-limits remained unchanged and no negative influence on the energy confinement as well as on the H-mode threshold was found.

Keywords: ASDEX Upgrade; High Z material; Impurity transport; Erosion and particle deposition

1. Introduction

At present, one of the most difficult design issues for ITER is the choice of the plasma facing materials, in particular for the divertor components [1]. Up to now beryllium or carbon are used as divertor materials in most of present-day tokamaks due to their low atomic charge. Both materials, however, have disadvantages, which might be unacceptable in a future fusion device [2]. Graphite suffers from an enhanced erosion by chemical processes even at low temperatures. Beryllium has a high physical sputtering yield, a low melting point and a high vapour pressure.

Tungsten, however, exhibits much more favourable properties with respect to erosion and other physical properties [2]. There is also good evidence that physical sputtering rates are lowered by prompt redeposition due to the gyro motion in the local magnetic field [3,4]. On the other hand, the high self-sputtering rates make the use of W only feasible at low temperature, high density divertor conditions [5]. Due to the high radiation power of W [6], its fractional abundance in the main plasma should be below 10^{-4} [7,8]. Recent experiments at TEXTOR with a tungsten test-limiter [9,10] show accumulation of W in Ohmic discharges for plasma densities above a critical value, whereas in discharges with an auxiliary heating power above a certain threshold no thermal instability at high densities due to the W-radiation is found. Alcator C-Mod, which operates at high densities with molybdenum first wall and divertor report no accumulation, but Mo-concentrations of about $2 \cdot 10^{-4}$ and a fraction of about 30% of the total radiation due to Mo in the plasma centre [11]. A more comprehensive compilation on the ongoing high Z experiments is found in a recent review [12]. To investigate the suitability of tungsten in a divertor tokamak under reactor relevant conditions and to compare it with the

* Corresponding author. Tel.: +49-89 3299 1899; fax: +49-89 3299 1812; e-mail: Neu@ipp.mpg.de.

PII S0022-3115(96)00586-7

operation with complete graphite first wall, W coated divertor tiles were mounted in the ASDEX Upgrade divertor. The major points of interest are the investigation of erosion and deposition processes as well as the transport of the tungsten into and inside the bulk plasma. The results of the surface analysis of exposed tungsten and graphite probes using ion beam techniques are described elsewhere in detail [13,14]. In this paper a first report of the results of spectroscopic investigations on the behavior of tungsten as well as the influence of the tungsten divertor on the plasma performance and on the other intrinsic impurities will be given.

2. The tungsten divertor

The tungsten-coated divertor in ASDEX Upgrade consists of a toroidal belt of tungsten tiles on the inner and outer target plate (Fig. 1). There are only a few graphite tiles for Langmuir probes and thermography left, representing less then 10% of the strike zone. In the toroidal direction the tiles are slightly tilted to achieve shadowed edges. An individual tile consists of a fine-grain graphite substrate (EK 98) coated with a 0.5 mm thick layer of tungsten. A 20 μm W/Re-multilayer (developed by Plansee AG) prevents the formation of carbides within the main tungsten layer and thus inhibits its embrittlement. Prototypes of the tiles were tested intensively by electron and ion beam irradiation. Both, the structure of the coatings and the tests of the tungsten tiles, were described in more detail elsewhere [15]. As a result of the tests the heat load on the tiles was limited to 7 MW/m^2. To raise confidence in the imposed load limit, fatigue tests at 7 MW/m^2 and 2 s with original tiles have been performed in parallel to the ongoing experiment. In the early phase of these tests, the coatings developed a network of microcracks, which affected only the uppermost surface region of the plasma sprayed tungsten layer and therefore did not diminish the thermal or mechanical performance of the coating. After 400 cycles, however, macrocracks were detected, which penetrated through the whole thickness of the tungsten layer and could lead to severe damage on tiles installed in the divertor of the tokamak.

3. Behavior of tungsten in plasma discharges

In ASDEX Upgrade up to now around 500 discharges with tungsten divertor were performed, over 300 of which were substantially auxiliary heated. The discharges comprise almost the full operational space of ASDEX Upgrade in regard to plasma current, density and auxiliary heating power. The power load on the target plates, which is deduced routinely from temperature measurements using a thermography camera [16], reached up to 6 MW/m^2 in a 7.5 MW neutral beam heated discharge. During ELMs (edge localized modes), these values reached up to 15 MW/m^2. Despite these power loads no damage to any of the tungsten tiles was observed up to now.

The tungsten flux in the divertor was monitored spectroscopically by a WI line at 400.8 nm using a scanning spectrometer-system viewing almost perpendicular onto the target plates [17]. During one discharge the strike zones on the outer as well as on the inner target plate could be scanned with the spectrometer several times during a discharge, allowing to record the spatial profile across the target plates. At the moment it is not possible to calculate the absolute W flux from the target plates from the mea-

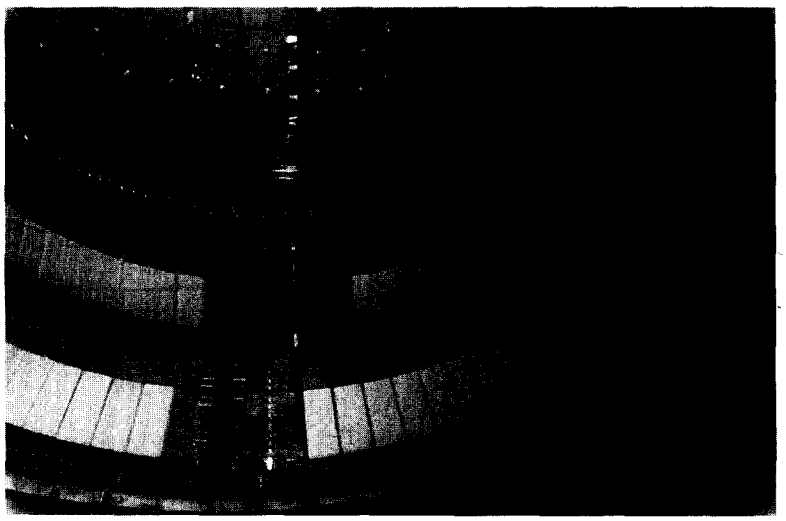

Fig. 1. The tungsten divertor in ASDEX Upgrade. The tungsten coated tiles were mounted on a toroidal ring at the outer and the inner strike zones. At the location of the Langmuir probes (front side) as well as for thermography (right side) graphite tiles were installed.

sured line intensities, since the ratio of ionisation rate to the excitation rate, the so called S/XB-value is not available. Nevertheless, the relative behavior of the W-fluxes under different discharge conditions should be reflected in the line emission, since the S/XB-value can be assumed to be almost constant for temperatures above 10 eV.

Erosion measurements with the divertor probe yield absolute erosion rates for single discharges [13]. By comparison with these erosion measurements, an in-situ calibration of the spectroscopic measurements will be performed.

In Fig. 2 the intensity of the WI-line is shown together with other plasma parameters. To enhance the sputtered flux the initial gas puffing is done with He, whereas during the NB-heating the valve was turned off. Two beams (5 MW) were switched on at 1.5 s, a third beam is added at 2.5 s. The CIII line intensity, measured above the divertor plates, indicates strong type I ELMs [18], whose frequency increases with heating power. Due to the beam fueling, the neutral gas flux density in the divertor, which is a measure for the neutral gas density and the line averaged density rise slowly. The time averaged electron temperatures, measured by Langmuir probes rise also with increasing heating power. In the Ohmic phases (before 1.5 s and after 3.6 s) the strike zone on the target plate moves away from the Langmuir probe, therefore no temperature is shown in these phases. The maximum WI intensity, shown in the uppermost part of the figure, rises clearly with increasing input power. The line of sight of the spectrometer is scanned across the outer target plates as described above, yielding also the spatial profiles of the WI spectral line. The details of the profiles are shown in

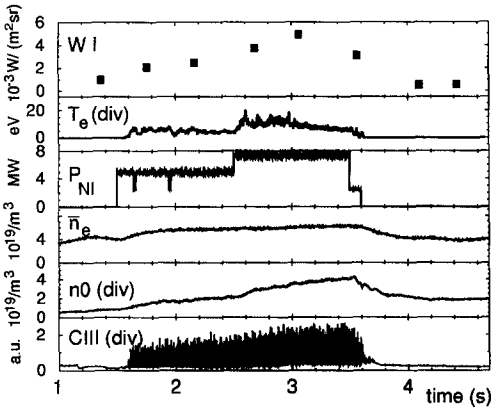

Fig. 2. Temporal behavior of the WI spectral line at 400.8 nm during the auxiliary heated 1 MA discharge #8021. The WI line intensity is measured by a periodical scan over the separatrix position. The squares indicate the maximum WI line intensity. Besides the WI intensity of the averaged electron temperature in the divertor, the NB power, the neutral gas flux density, the line averaged density and the CIII line intensity from the divertor are shown.

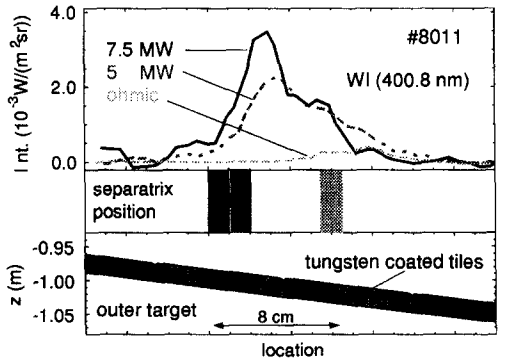

Fig. 3. Spatial profile of the WI spectral line over the outer target plate from the auxiliary heated discharges #8011 during different heating phases. The tungsten target is shown schematically in the lower part of the figure, the corresponding position of the separatrix is indicated by a vertical bar.

Fig. 3. The profiles are averaged over the two scans during the phases with almost constant plasma parameters (Ohmic: 3.8–4.6 s, 5 MW NBI: 1.6 s–2.4 s and 7.5 MW NBI: 2.5–3.3 s). The outer target plate, with the tungsten coated tiles and the corresponding separatrix position, which is indicated by a vertical bar, is shown in the lower part of the picture. The intensity is localized in the scrape off layer and the shifts of the separatrix due to the changes in the plasma pressure are reflected in the data.

In Ohmic discharges an even clearer dependence of the WI intensity on the electron temperatures in the divertor is found. Fig. 4 demonstrates the behavior of the WI line for different densities and constant heating power. In an Ohmic 600 kA discharge the line averaged density was ramped up

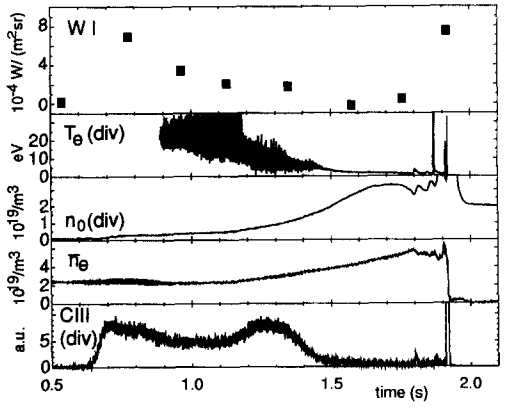

Fig. 4. Temporal behavior of the WI spectral line during the 600 kA Ohmic density limit discharge #8021. Besides the WI line intensity (squares), which is again obtained by a periodical scan over the separatrix position, the electron temperature in the divertor, the neutral gas flux density, the line averaged density and the CIII line intensity from the divertor are shown.

from $2.5 \cdot 10^{19}/m^3$ to $5.6 \cdot 10^{19}/m^3$ (density limit). Whereas for $\bar{n}_e = 2.5 \cdot 10^{19}/m^3$ the WI intensity could be clearly seen above the background, it disappears for $\bar{n}_e = 4 \cdot 10^{19}/m^3$ where the plasma detaches from the divertor ($t \approx 1.5$ s) as can be seen from the electron temperature which decreases far below 10 eV. The temperature is only shown for $t > 0.9$ s, where the separatrix is located at the position of the Langmuir probe. For comparison also a CIII line measured above the divertor plates is shown. It rises rapidly when the plasma fan strikes the outer target plate and disappears also with the beginning of the detached phase. The peak at the end of the discharge, visible in the WI as well as in the CIII intensity is caused by the vertical instable plasma which moves into the divertor at the moment of the density limit disruption.

In discharges with high density and high auxiliary heating power no enhanced sputtering through seeded neon was found and the WI intensity stayed below the detection limit. This is similar to observations at TEXTOR [19], where no rise of the WI intensity was found, indicating that the enhanced sputtering capability of the neon ions is at least compensated by the reduced temperature at the plasma boundary.

In the plasma centre an array of spectral lines at 5 nm emitted by ionisation states around W XXX was monitored with a VUV spectrometer viewing in the equatorial plane [20,5]. The spectrometer was cross-calibrated previously by comparison of the measured radiation with the theoretical radiation power [6] after tungsten laser ablation [21]. The accuracy of this method is estimated from extensive W-laser ablation experiments [22] to be within a factor of 2. The detection limit for the W-concentration ($c_W = n_W/n_e$) is better than 10^{-5}, depending on the actual plasma parameters. Over 90% of the investigated 300 discharges, Ohmic as well as L- and H-Mode, show concentrations in the range or below $2 \cdot 10^{-5}$. Fig. 5 shows the concentration of all investigated discharges of this experimental campaign. The concentrations in Ohmic discharges are shown as circles and in auxiliary heated discharges as triangles. Open symbols represent discharges where the concentration is below the detection limit and finally the orientation of the triangles indicates heating powers above (peak to the top) or below (peak to the bottom) 5 MW. Boronization procedures which are indicated by vertical bars, were performed routinely as in the graphite divertor case. They do not seem to have a big influence on the W concentrations, although the effect is not completely clear due to the W-detection limit. In contrast to observations at TEXTOR [19] no enhanced W concentrations were found in neon seeded discharges, probably due to a more effective reduction of the W source in the divertor.

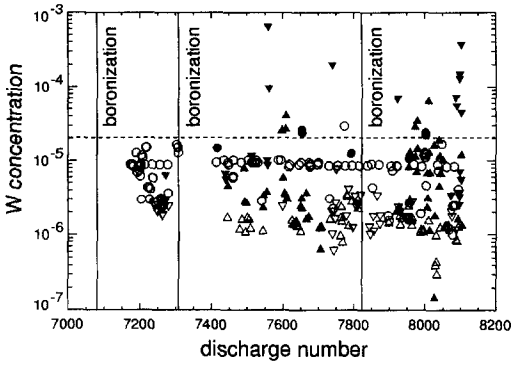

Fig. 5. Maximum concentrations of tungsten deduced from the W line array at 5 nm. The concentrations in ohmic discharges are shown as circles, in auxiliary heated discharges as triangles. Open symbols represent discharges where the concentration is below the detection limit and the orientation of the triangles indicates heating powers below (▽) or above (△) 5 MW. Boronization procedures are indicated by vertical bars.

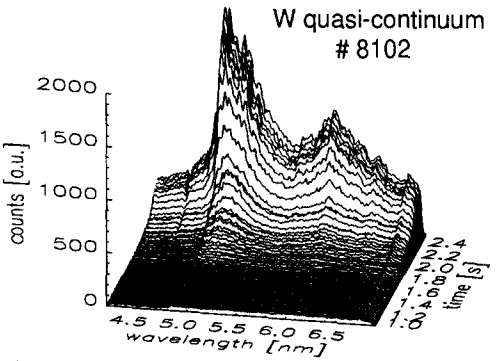

Fig. 6. Temporal behavior of the W quasicontinuum at 5 nm during the 600 kA auxiliary heated discharge #8102. The line averaged density was about $6 \times 10^{19}/m^3$, the NB heating power was 2.3 MW. The accumulation starts shortly after neutral beam injection at 1.5 s and saturates at about 2.6 s.

No clear relation between the flux measurements and the extracted concentrations is found, indicating that the transport of W into and within the plasma plays a major role for the W content in a specific plasma discharge. This is elucidated in the few discharges, where W-concentrations above 10^{-4} occurred, although no enhanced W-flux from the target plates was observed. Strong accumulation of W occurred only with low heating power and low energy of the neutral beams. Since in these discharges the density was kept also low, the heating profile of the beams is not significantly changed, whereas fast ion losses and the resulting electric field may play a significant role. Fig. 6 shows the strong increase of the W quasicontinuum in a 1.5 MW NB heated discharge. In the Ohmic phase ($t <$ 1.5 s) no tungsten lines are visible, whereas after the beams were turned on, the quasicontinuum rises quickly. These discharges were often characterized by a strong central mode activity and the absence of sawteeth, a condition which generally is found to favour the accumulation of impurities. Additionally, the temperature profiles

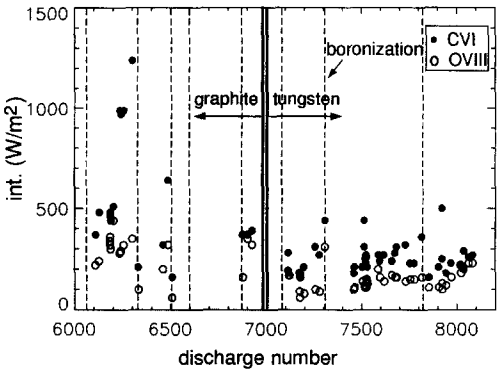

Fig. 7. Intensity of the C VI (full circles) and O VIII (open circles) Lyman- and spectral lines from ohmic standard discharges (IP 600 kA). The broad vertical bar marks the change from graphite to tungsten tiles in the divertor, whereas the dashed vertical lines represent the vessel conditioning by boronization.

were flattened and the density profiles became more peaked. Whether this is a result of the accumulation or a prerequisite for the neoclassical inward drifts is not yet clear at the moment.

4. Plasma performance

The influence of the tungsten divertor on the other intrinsic impurities and on the global plasma behavior was found to be negligible with the exception of those rare discharges, where accumulation of tungsten occurred.

The carbon and oxygen content in Ohmic standard discharges is monitored routinely by two crystal spectrometers [23]. The intensities of the Lyman α spectral lines of the H-like ions were comparable to the discharges of the preceding experimental campaign (Fig. 7). A strong reduction especially of the oxygen radiation is found as usual in both periods after boronization of the vessel. These results are in line with former observations at ASDEX Upgrade: A large amount of the C impurity is produced by chemical erosion from the inner graphite heat shield [24]. Density limit discharges were performed at the beginning of every day of operation. No significant change in density limit was observed. In a few discharges also the β-limit was explored. The results were identical to former investigations [25]. Although no complete statistical evaluation of all relevant discharges was performed up to now, the evaluation of sample discharges shows that there is no negative influence of the tungsten divertor on the energy confinement as was well as on the H-mode threshold.

5. Summary and discussion

First results of the operation with a full toroidal tungsten divertor were reported. The discharges performed up to now comprise almost the full operational space of the ASDEX Upgrade tokamak. The WI flux in the divertor as well as a line array from ionisation states around WXXX in the plasma centre were observed routinely. A strong dependence of WI intensity on the divertor electron temperatures is found. For detached plasmas no WI line emission can be detected, indicating that there is almost no erosion. Over 90% of the investigated discharges show concentrations below $2 \cdot 10^{-5}$.

Now no clear relation between the WI intensity in the divertor and the W radiation in the main plasma is found. Enhanced W concentrations in the plasma seem to result from an improved W confinement in the core rather than from enhanced tungsten fluxes from the divertor because they are only found in low input power auxiliary heated plasmas with relatively low power load on the divertor tiles. Strong accumulation of W was only found in the special case of low energy, low power neutral beam injection. Other accumulating regimes identified at ASDEX [26] showed no accumulation (pellet fueling) or were not yet investigated (quiescent H-modes, Counter NBI). An individual examination of the discharges with enhanced W concentrations will be performed in the near future to clarify the reasons and circumstances of accumulation.

In all the discharges without tungsten accumulation, which are by far the most, the influence on the main plasma parameters was negligible. The density- as well as the β-limit remained unchanged and no deterioration of the energy confinement occurs. Statistical evaluations of a large number of discharges are under way to buttress the findings about confinement and H-mode thresholds.

Long term measurements on the tiles show a significant dilution of W at the surface by B, C and O [13]. Nevertheless the fraction of W at the surface is still about 50%, representing a significant potential W source. Since it is planned to use Be, C and W as plasma facing materials in ITER [27], a similar situation could be expected there. Moreover, Alcator C-Mod, where the whole first wall components are made of Mo, reports also comparable concentrations of carbon due to an initial contamination of the Mo tiles [11].

The above presented results, especially for high power discharges, seem rather encouraging for the utilization of high Z plasma facing components in a future device.

References

[1] G. Janeschitz, K. Borras, G. Federici, Y. Igitkhanov, A. Kukushkin et al., J. Nucl. Mater. 220–222 (1995) 73.
[2] C. García-Rosales, J. Nucl. Mater. 211 (1994) 202.
[3] D. Naujoks, J. Roth, K. Krieger, G. Lieder and M. Laux, J. Nucl. Mater. 210 (1994) 43.
[4] J. Roth, D. Naujoks, K. Krieger, A. Field, G. Lieder et al., J. Nucl. Mater. 220–222 (1995) 231.
[5] D. Naujoks, K. Asmussen, M. Bessenrodt-Weberpals, S. Deschka, R. Dux et al., Nucl. Fusion, to be published.

[6] D. Post, R. Jensen, C. Tarter, W. Grasberger and W. Lokke, At. Data Nucl. Data Tables 20 (1977) 397.
[7] R. Jensen, D. Post and D. Jassby, Nucl. Sci. Eng. 65 (1978) 282.
[8] T. Tanabe, N. Noda and H. Nakamura, J. Nucl. Mater. 196–198 (1992) 11.
[9] V. Philipps, M. Tokar, A. Prospieszczyk, U. Kögler, R. Koslowski et al., in: Europhysics Conference Abstracts, Proc. 22nd EPS Conference on Controlled Fusion and Plasma Physics, Bournemouth, 1995 (Petit-Lancy, 1995) EPS, 19C(II) pp. 321–324.
[10] G. Van Oost, A. Messiaen, V. Philipps, R. Koch, A. Krämer-Flecken et al., in: Europhysics Conference Abstracts, Proc. 22nd EPS Conference on Controlled Fusion and Plasma Physics, Bournemouth, 1995 (Petit-Lancy, 1995) EPS, 19C(II) pp. 345–348.
[11] J. Goetz, B. Lipschultz, M. Graf, C. Kurz, R. Nachtrieb et al., J. Nucl. Mater. 220–222 (1995) 971.
[12] N. Noda, V. Philipps and R. Neu, J. Nucl. Mater. (1996), to be published.
[13] K. Krieger, J. Roth, A. Annen, W. Jacob, C. Pitcher et al., J. Nucl. Mater. (1996), to be published.
[14] K. Krieger, V. Rohde, R. Schwörer, K. Asmussen, C. García-Rosales et al., J. Nucl. Mater. (1996), to be published.
[15] C. García-Rosales, S. Deschka, W. Hohenauer, R. Duwe, E. Gauthier et al., Nucl. Fusion Technol., to be published.
[16] A. Herrmann, W. Junker, K. Günther, S. Bosch, M. Kaufmann et al., Plasma Phys. Control. Fusion 37 (1995) 17.
[17] A.R. Field, J. Fink, R. Dux, G. Fussman, U. Wenzel et al., Rev. Sci. Instrum. 66 (1995) 5433.
[18] H. Zohm, Plasma Phys. Control. Fusion 38 (1995) 105.
[19] Y. Ueda, T. Tanabe, V. Phillips, L. Könen, A. Pospieszczyk et al., J. Nucl. Mater. 220–222 (1995) 240.
[20] R. Neu, K. Asmussen, R. Dux, P. Ignacz, M. Bessenrodt-Weberpals et al., in: Europhysics Conference Abstracts, Proc. 22nd EPS Conference on Controlled Fusion and Plasma Physics, Bournemouth, 1995, ed. B. Keen, P. Stott and J. Winter (Geneva, 1995), EPS, 19C(I) pp. 65–68.
[21] K. Asmussen et al., to be published.
[22] K. Asmussen, Technical Report 10/2, IPP (Garching, Germany, 1996).
[23] R. Neu, K. Asmussen, G. Fußmann, P. Geltenbort, G. Janeschitz et al., Rev. Sci. Instrum. 67 (1996) 1829.
[24] A. Kallenbach, R. Neu, W. Poschenrieder and ASDEX Upgrade Team, Nucl. Fusion 34 (1994) 1557.
[25] H. Zohm, M. Marschek, G. Pautasso, M. Schittenhelm, S. Sesnic et al., Plasma Phys. Control. Fusion 37 (1995) A313.
[26] G. Fussmann, J. Hofmann, G. Janeschitz, K. Krieger, E. Müller et al., J. Nucl. Mater. 162–164 (1994) 14.
[27] R. Parker et al., J. Nucl. Mater. (1996), to be published.